Sparse Seismic Time-Variant Deconvolution Using Q Attenuation Model

Deborah Pereg and Israel Cohen, Technion – Israel Institute of Technology, and Anthony A. Vassiliou, GeoEnergy*

SUMMARY

We consider the problem of recovering the underlying reflectivity signal from its seismic trace, taking into account the attenuation and dispersion propagation effects of the reflected waves in noisy environments. We introduce an efficient method to perform seismic time-variant deconvolution based on the earth Q-model. We present theoretical bounds on the recovery error, and on the localization error. It is shown that the solution consists of recovered spikes, which are relatively close to spikes in the true reflectivity signal. In addition, any redundant spike in the solution, which is far from the correct support, has a small energy. The proposed method is demonstrated using synthetic and real data examples.

INTRODUCTION

Sparse seismic deconvolution has attracted much research recently. Previous works tried to solve the seismic deconvolution problem by separating the seismic 2D image into independent vertical one-dimensional (1D) deconvolution problems. The wavelet is modeled as a 1D time-invariant signal in both horizontal and vertical directions. Each reflectivity channel (column) appears in the vertical direction as a sparse spike train where each spike is a reflector that corresponds to a boundary between two layers in the ground. Then, each reflectivity channel is estimated from the corresponding seismic trace observation apart from the other channels (Berkhout, 1986; Ulrych, 1971; Taylor et al., 1979; Riel and Berkhout, 1985; Nguyen and Castagna, 2010; Zhang and Castagna, 2011; Gholami and Sacchi, 2012).

Utilization of sparse seismic deconvolution methods based on ℓ_1 minimization can yield stable reflectivity solutions (Riel and Berkhout, 1985; Nguyen and Castagna, 2010; Gholami and Sacchi, 2012; Pham et al., 2014; Repetti et al., 2015). These ℓ_1-type methods and their resolution limits are studied thoroughly in Signal Processing and Statistics (Duval and Peyré, 2015; Donoho, 1992; Dossal and Mallat, 2005; Fernandez-Granda, 2013; Candès and Fernandez-Granda, 2013a,b; Bendory et al., 2016b,a; Tibshirani, 2013; Efron et al., 2004).

Many deconvolution methods rely on a model which does not take into consideration time-depth variations in the waveform. However, the wave absorption effects are not always negligible as the conventional assumption claims. Seismic inverse Q-filtering (Kjartansson, 1979; Gelius, 1987; Hale, 1981; Wang, 2008) aims to compensate for the velocity dispersion and energy absorption which causes phase and amplitude distortions of the propagating and reflected acoustic waves. The process of inverse Q filtering consists of amplitude compensation and phase correction which enhance the resolution and increase the signal-to-noise ratio (SNR). Yet, this process is generally computationally expensive and sometimes even impractical.

In this paper, which summarizes some of the results in Pereg and Cohen (2017), we introduce a robust algorithm for recovery of the underlying reflectivity signal from the seismic data without a pre-processing stage of inverse Q filtering. The recovery is conducted by solving a convex optimization problem, which takes into consideration a time-variant signal model. In addition we discuss the following questions: To what accuracy can we recover each reflectivity spike? How does this accuracy depend on the noise level, the amplitude of the spike, the medium Q constant and the wavelet? We show that the recovery error is proportional to the noise level. Experimental results for synthetic and real seismic data demonstrate the improved performance of the proposed method.

SIGNAL MODEL

Reflectivity model

We assume the earth structure is stratified, so that reflections are generated at the boundaries between different impedance layers. Therefore, each 1D channel (column) in the unknown 2D reflectivity signal can be formulated as a sparse spike train

$$x[k] = \sum_m c_m \delta[k - k_m], \tag{1}$$

where $\delta[k]$ denotes the Kronecker delta function and $\sum_m |c_m| < \infty$ (Ricker, 1940). The set of delays $K = \{k_m\}$ and the real amplitudes $\{c_m\}$ are unknown. In noisy environments we consider a discrete seismic trace of the form

$$y[k] = \sum_m c_m g_{\sigma,m}[k - k_m] + n[k], \quad \|n\|_1 \leq \delta, \tag{2}$$

where $\{g_{\sigma,m}\}$ is a known set of kernels (pulses) for a possible set of time delays $K = \{k_m\}$, and a known scaling parameter $\sigma > 0$, and $n[k]$ is additive noise with $\|n\|_1 = \sum_k |n[k]| \leq \delta$. Our objective is to estimate the true support $K = \{k_m\}$ and the spikes' amplitudes $\{c_m\}$ from the observed seismic trace $y[k]$.

Earth Q model

We assume a source waveform $s(t)$ defined as the real-valued Ricker wavelet

$$s(t) = \Big(1 - \frac{1}{2}\omega_0^2 t^2\Big) \exp\Big(-\frac{1}{4}\omega_0^2 t^2\Big), \tag{3}$$

where ω_0 is the most energetic (dominant) radial frequency, which is related to the scaling parameter by $\sigma = \omega_0^{-1}$. Given a travel time t_m, the reflected wave can be modeled as (Wang, 2002)

$$u(t) = \mathrm{Re}\Big\{\frac{1}{\pi}\int_0^\infty S(\omega)\exp[j(\omega t - \kappa r(\omega))]d\omega\Big\}, \tag{4}$$

where $S(\omega)$ is the Fourier transform of the source waveform $s(t)$,

$$\kappa r(\omega) \triangleq \Big(1 - \frac{j}{2Q}\Big)\left|\frac{\omega}{\omega_0}\right|^{-\gamma}\omega t_m, \tag{5}$$

$$\gamma \triangleq \frac{2}{\pi}\tan^{-1}\left(\frac{1}{2Q}\right) \approx \frac{1}{\pi Q}, \tag{6}$$

and Q is the medium quality factor, which is assumed to be frequency independent (Kjartansson, 1979). Kjartansson (1979) defined Q as the portion of energy lost during each cycle or wavelength.

Therefore, the expression of the earth Q filter consists of two exponential operators that express the phase effect (caused by velocity dispersion) and the amplitude effect (caused by energy absorption)

$$U(t-t_m,\omega) = U(t,\omega)\exp\Big(-j\left|\frac{\omega}{\omega_0}\right|^{-\gamma}\omega t_m\Big)\exp\Big(-\left|\frac{\omega}{\omega_0}\right|^{-\gamma}\frac{\omega t_m}{2Q}\Big). \tag{7}$$

Summing these plane waves, we get the time-domain seismic signal

$$u(t-t_m) = \frac{1}{2\pi}\int U(t-t_m,\omega)d\omega. \tag{8}$$

We can now define the known set of kernels (pulses) $\{g_{\sigma,m}\}$ for the seismic setting by

$$g_{\sigma,m}(t-t_m) = u(t-t_m)|_{\sigma=\omega_0^{-1}}. \tag{9}$$

SPARSE SEISMIC DECONVOLUTION

Admissible Kernels and Separation Constant

To be able to quantify the waves decay and concavity we recall two definitions from previous works (Bendory et al., 2016b,a):

Definition 2.1 A kernel g is **admissible** if it has the following properties:

1. $g \in \mathbb{R}$ is real and even.
2. Global Property: There exist constants $C_l > 0, l = 0,1,2,3$, such that $\left|g^{(l)}(t)\right| \leq \frac{C_l}{1+t^2}$, where $g^{(l)}(t)$ denotes the l^{th} derivative of g.
3. Local Property: There exist constants $\varepsilon, \beta > 0$ such that
   (a) $g(t) > 0$ for all $|t| \leq \varepsilon$ and $g(\varepsilon) > g(t)$ for all $|t| \geq \varepsilon$.
   (b) $g^{(2)}(t) < -\beta$ for all $|t| \leq \varepsilon$.

In other words, the kernel and its first three derivatives are decaying fast enough, and the kernel is concave near its midpoint.

Definition 2.2 A set of points $K \subset \mathbb{Z}$ is said to satisfy **the minimal separation condition** for a kernel dependent $\nu > 0$, a given scaling $\sigma > 0$ and a sampling spacing $1/N > 0$ if

$$\min_{k_i,k_j\in K, i\neq j}\left|k_i - k_j\right| \geq N\nu\sigma$$

where $\nu\sigma$ is the smallest time interval between two reflectors with which we can still recover two distinct spikes, and ν is called the separation constant.

Figure 1 shows an example of the attenuating wavelets $g_{\sigma,m}(t)$ and their derivatives, $g^{(1)}_{\sigma,m}(t)$ and $g^{(2)}_{\sigma,m}(t)$ for $Q = 125$, $t_m = 100, 250, \ldots, 1900$ms (increments of 150ms), and $\omega_0 = 100\pi$ (50Hz). The pulses and their derivatives are shifted to the origin so that it can be seen that there there are common values of ε and β for all the sequence of kernels $g_{\sigma,m}(t)$. The kernels $g_{\sigma,m}(t)$ are not symmetric, but remain flat at the origin, i.e., $g^{(1)}_{\sigma,m}(0) \approx 0$. So it can be said that the kernels $g_{\sigma,m}(t)$ are approximately admissible kernels.

Sparse Deconvolution and Error Bound

The recovery of the seismic reflectivity could be achieved by solving the following optimization problem: Let y be of the form of (2) and let $\{g_{\sigma,m}\}$ be a set of admissible kernels. If K satisfies the separation condition for $N > 0$ then the solution $\hat{x}$ of

$$\min_{x\in\ell_1(\mathbb{Z})}||x||_1 \quad \text{subject to} \quad ||y[k] - \sum_m c_m g_{\sigma,m}[k-k_m]||_1 \leq \delta \tag{10}$$

satisfies

$$||\hat{x}-x||_1 \leq \frac{4\rho}{\beta\gamma_0}\delta \tag{11}$$

where

$$\rho \triangleq \max\left\{\frac{\gamma_0}{\varepsilon^2}, (N\sigma)^2\alpha_0\right\}$$

$$\alpha_0 = \max_m g_{\sigma,m}(0), \quad \gamma_0 = \min_m g_{\sigma,m}(0).$$

The dependance of x on the time k is not written for simplicity.

This result guarantees that under the separation condition, a signal of the form of (2), can be recovered by solving the ℓ_1 optimization problem formulated in (10). Moreover, a theoretical analysis of the recovered solution (Pereg and Cohen, 2017) ensures that the error is bounded by a relatively small value, which depends mainly on the noise level and on the attenuation of the wavelets and is expressed through the parameters Q and β.

In the noiseless case where $\delta = 0$, the recovery is perfect. One would probably expect that the recovered solution would slightly deviate from the true one, yet this is not the case. This result does not depend on whether the spikes amplitude are very small or very large.

If $\gamma_0 = \alpha_0$, we have the time-invariant case

$$||\hat{x}-x||_1 \leq \frac{4\delta}{\beta}\max\left\{\frac{1}{\varepsilon^2}, (N\sigma)^2\right\}.$$

As expected, in the time-invariant case our result reduces into previous work results (Bendory et al., 2016b,a). The recovery error is proportional to the noise level δ, and small values of β (flat kernels) result in larger errors.

In the time-variant setting, most cases comply with $\gamma_0/\varepsilon^2 < (N\sigma)^2\alpha_0$. Then, the recovery error is bounded by

$$||\hat{x}-x||_1 \leq \frac{4(N\sigma)^2}{\beta}\frac{\alpha_0}{\gamma_0}\delta.$$

A smaller Q (which corresponds to a stronger degradation) results in higher α_0/γ_0 ratio and smaller β values. We will hereafter refer to the ratio α_0/γ_0 as the degradation ratio. Hence, the bound on the error in a time-variant environment implies that the error increases as Q gets smaller, which corresponds

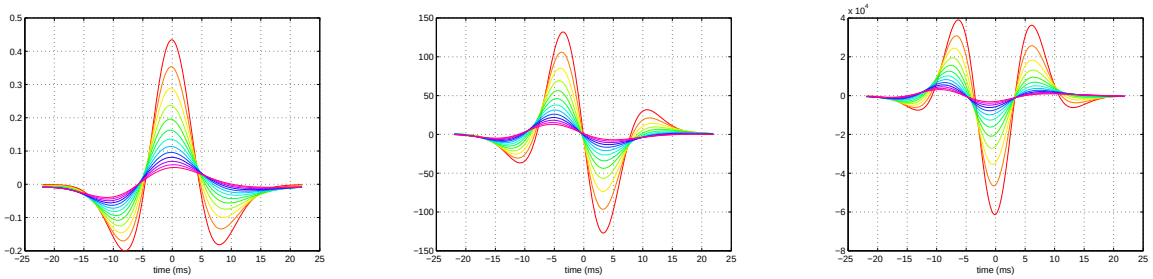

(a) (b) (c)

Figure 1: Centered synthetic reflected wavelets and their derivatives, $Q = 125, \omega_0 = 100\pi$ (50Hz) (a) $g_{\sigma,m}(t)$; (b) $g^{(1)}_{\sigma,m}(t)$; (c) $g^{(2)}_{\sigma,m}(t)$.

to a higher degradation ratio. As in the time-invariant case, the error is linear with respect to the noise level δ. Also, the error is sensitive to the flatness of the kernel near the origin. Namely, small β results in an erroneous recovery.

Resolution Bound

Assume $\hat{x}[k] = \sum_m \hat{c}_m \delta[k - \hat{k}_m]$ is the solution of (10) where $\hat{K} \triangleq \{\hat{k}_m\}$ is the support of the recovered signal. Let y be of the form of $y[k] = \sum_m c_m g_{\sigma,m}[k - k_m] + n[k],\ \|n\|_1 \le \delta$, and let $\{g_{\sigma,m}\}$ be a set of admissible kernels with two common parameters $\varepsilon, \beta > 0$, with $\varepsilon \ge \tilde{\varepsilon} = \sqrt{\frac{\alpha_0}{C_2 + \beta/4}}$. If K satisfies the separation condition for $N > 0$, then the solution $\hat{x}$ satisfies:

1. $$\sum_{\hat{k}_m \in \hat{K}: |\hat{k}_m - k_m| > N\varepsilon, \forall k_m \in K} |\hat{c}_m| \le \frac{2D_3\alpha_0}{\beta\varepsilon^2}\delta$$

   Any redundant spike in $\hat{K}$ which is far from the correct support K will for sure have small energy.

2. For any $k_m \in K$ if $|c_m| \ge D_4$, then there exist $\hat{k}_m \in \hat{K}$ such that

   $$(\hat{k}_m - k_m)^2 \le \frac{2D_3(N\sigma)^2\alpha_0}{\beta\left(|c_m| - D_4\right)}\delta.$$

   where

   $$D_4 = \frac{2\delta}{\beta}\left(\frac{2\rho}{\gamma_0} + D_3\alpha_0 \max\left\{\frac{1}{\varepsilon^2}, \frac{C_{2,m}}{(N\sigma)^2 g_m(0)}\right\}\right),$$

   $$D_3 = \frac{3\nu^2(3\gamma_2\nu^2 - \pi^2\tilde{C}_2) + \frac{12\pi^2\tilde{C}_1^{\,2}}{\beta\gamma_0}(1 + \frac{\pi^2}{6\nu^2})\rho}{(3\gamma_2\nu^2 - \pi^2\tilde{C}_2)(3\gamma_0\nu^2 - 2\pi^2\tilde{C}_0)}.$$

   and

   $$\tilde{C}_l = \max_m C_{l,m},\ l = 0, 1, 2, 3.$$

This implies that for any $k_m \in K$ with sufficiently large amplitude c_m, under the separation condition, the recovered support location $\hat{k}_m \in \hat{K}$ is close to the original one. The solution $\hat{x}$ consists of a recovered spike near any spike of the true reflectivity signal.

EXPERIMENTAL RESULTS

Synthetic Data

We conducted various experiments in order to confirm the theoretical results. To solve the ℓ_1 minimization in (10) we used CVX (Grant and Boyd, 2014).

We generate a synthetic reflectivity column, with a sampling interval $Ts = 4$ms. The reflectivity is statistically modeled as a zero-mean Bernoulli-Gaussian process (Kormylo and Mendel, 1982). The support was drawn from a Bernoulli process with $p = 0.2$ of length $L_r = 176$ taps, and the amplitudes were drawn from an i.i.d normal distribution with standard deviation $v = 10$. Then, we create the synthetic seismic trace in a noise-free environment, and try to recover the reflectivity by solving (10).

Figure 2 presents the recovery error $||\hat{x} - x||_1$ as a function of the noise level δ for different Q values - $Q = \infty, 500, 200, 100$. Under the separation condition, the minimum distance between two spikes satisfies the minimal separation condition. The reflectivity is shown in Fig. 3(a). The initial wavelet was a Ricker wavelet with $\omega_0 = 140\pi$, i.e., 70Hz.

Two seismic traces with SNR= ∞ and SNR= 15.5dB, are shown in Fig. 3(b) and Fig. 3(c), respectively. The recovered signals from these traces are shown in Fig. 3(d) and Fig. 3(e), respectively. As can be seen in Fig. 3, the error is linear with respect to the noise. This implies that the bound we derived is reasonable. The theoretical bound is always greater or equal to the empirical error. As Q gets smaller, β - which is common to all reflected pulses - becomes significantly smaller. Hence, the theoretical bound slope becomes significantly larger compared with the empirical one. It can be seen also in the experimental results that as Q gets smaller the error gets bigger. Table 1 presents the theoretical and practical parameters.

Real Data

We applied the proposed method, to real seismic data from a small land 3D survey in North America (courtesy of GeoEnergy Inc., TX) of size 380×160, shown in Fig. 4(a). The time interval is 2ms. Assuming an initial Ricker wavelet with $\omega_0 = 140\pi$ (70Hz). We estimated $Q = 80$ using common midpoints (CMP) as described in Zhang and Ulrych (2002). Then,

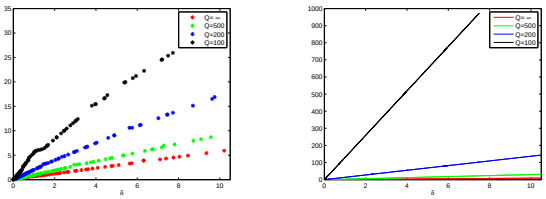

(a) (b)

Figure 2: Recovery error $||\hat{x}-x||_1$ as a function of noise level δ for $Q=\infty, 500, 200, 100$. (a) Experimental results ; (b) Theoretical bounds.

Q	$\frac{\alpha_0}{\gamma_0}$	β	$\frac{4(N\sigma)^2}{\beta}\frac{\alpha_0}{\gamma_0}$	estimated slope
∞	1	1.5	0.862	0.567
500	1.75	0.77	2.94	0.89
200	3.8	0.36	13.67	1.71
100	9.44	0.094	129.7	3.53

Table 1: Synthetic example. Theoretical and estimated parameters: Q, degradation ratio α_0/γ_0, β, theoretical bound slope $4(N\sigma)^2\alpha_0/\beta\gamma_0$ computed from known parameters, and estimated slope computed from the experimental results in Fig. 2(a).

using (6)-(11) we estimated all possible kernels and solved (10) using CVX (Grant and Boyd, 2014).

The recovered reflectivity section is shown in Fig. 4(c). Visually analyzing this reflectivity section, it can be seen that the layer boundaries in the estimate are clear and quite continuous and smooth. Since the ground truth is unknown, in order to measure the accuracy in the locations and amplitudes of the recovered reflectivity spikes, we compute the correlation coefficient between the reconstructed data and the given seismic data. In this example we have $\rho_{s,\hat{s}} = 0.967$, which indicates that the reflectivity is estimated with very high precision. Figure 4(b) shows the estimated reflectivity considering a time-invariant model, using Sparse Spike Inversion (SSI) (Taylor et al., 1979). It can be seen, especially in the lower (deeper) half of the image, that the proposed method produces much clearer results, since it takes into account the attenuating and broadening nature of the waves as they travel further into the ground and back. Moreover, in terms of correlation coefficients, for SSI we have $\rho_{s,\hat{s}} = 0.89$, implying that a time-varying model indeed yields better results.

CONCLUSIONS

We have presented a seismic deconvolution algorithm under a time-variant model. The algorithm both promotes sparsity of the solution and also takes into consideration attenuation and dispersion of the wavelet. The deconvolution results are demonstrated on synthetic and real data, under sufficiently high SNR. We derived a bound on the ℓ_1 recovery error and observed that the error increases as Q gets smaller. As in the time-invariant case, the error is proportional to the noise level. Also, the error is sensitive to the flatness of the kernel near the

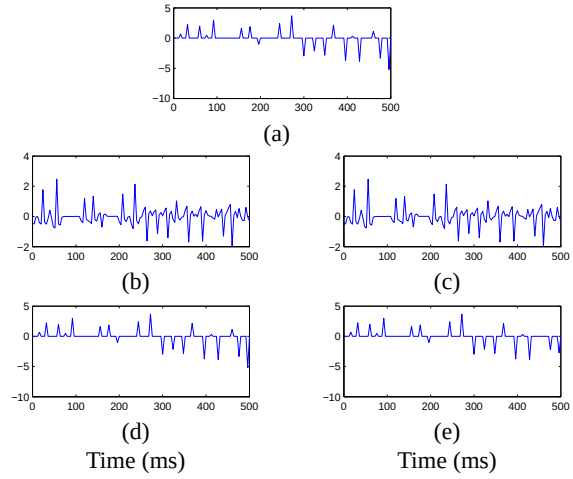

Figure 3: 1D synthetic tests of (a) True reflectivity. (b),(c) Synthetic traces with 50 Hz Ricker wavelet and SNR$=\infty, 15.5$ dB, respectively, $Q=200$. (d),(e) Recovered reflectivity signals.

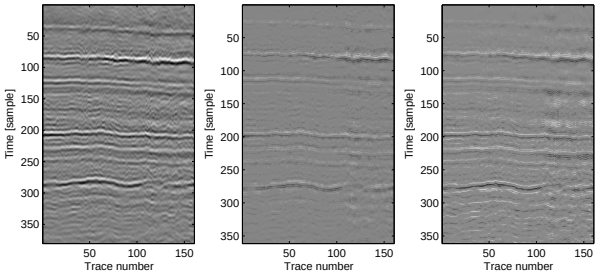

Figure 4: Real data deconvolution results: (a) Real seismic data (b) Estimated reflectivity - time-invariant model (SSI) (c) Estimated reflectivity - time-variant model.

origin. Simulation results confirm the theoretical bound. We also showed that under the separation condition, for any spike with large-enough amplitude the recovered support location is close to the original one. The solution consists of a recovered spike near every spike of the true reflectivity signal. Any redundant spike in the recovered signal, which is far from the correct support, has small energy.

REFERENCES

Bendory, T., S. D. A. Bar-Zion, and A. Feuer, 2016a, Stable support recovery of stream of pulses with application to ultrasound imaging: IEEE transaction on signal processing, **64**, 3750 – 3759.

Bendory, T., S. Dekel, and A. Feuer, 2016b, Robust recovery of stream of pulses using convex optimization: Journal of mathematical analysis and applications, **442**, 511–536.

Berkhout, A., 1986, The seismic method in the search for oil and gas: current techniques and future development: proceedings of the IEEE, **74**, 1133–1159.

Candès, E. J., and C. Fernandez-Granda, 2013a, Super-resolution from noisy data: Journal of Fourier Analysis and Applications, **19**, 1229–1254.

———, 2013b, Towards a mathematical theory of superresolution: Communications on Pure and Applied Mathematics.

Donoho, D. L., 1992, Super-resolution via sparsity constraints: SIAM J. Math. Anal., **23**, 1309–1331.

Dossal, C., and S. Mallat, 2005, Sparse spike deconvolution with minimum scale: SPARS, 123–126.

Duval, V., and G. Peyré, 2015, Exact support recovery for sparse spikes deconvolution: Foundations of Computational Mathematics, 1–41.

Efron, B., T. Hastie, I. Johnstone, and R. Tibshirani, 2004, Least angle regression: Annals of Statistics, **32**, 407–499.

Fernandez-Granda, C., 2013, Support detection in super-resolution: Proceedings of SampTA, 145–148.

Gelius, L., 1987, Inverse Q filtering. a spectral balancing technique: Geophysical Prospecting, 656–667.

Gholami, A., and M. D. Sacchi, 2012, A fast and automatic sparse deconvolution in the presence of outliers: IEEE Trans. Geosci. Remote Sens., **50**, 4105–4116.

Grant, M., and S. Boyd, 2014, CVX: Matlab software for disciplined convex programming: version 2.1.

Hale, D., 1981, An inverse Q filter: Stanford Exploration Project report, 231–243.

Kjartansson, E., 1979, Constant Q-wave propagtion and attenuation: Journal of Geophysical Research, 4737–4747.

Kormylo, J., and J. Mendel, 1982, Maximum likelihood detection and estimation of Bernoulli-Gaussian processes: IEEE Trans. Information Theory, **28**, 482–488.

Nguyen, T., and J. Castagna, 2010, High resolution seismic reflectivity inversion: Journal of Seismic Exploration, **19**, 303–320.

Pereg, D., and I. Cohen, 2017, Seismic signal recovery based on earth Q model: to apear in Signal Processing.

Pham, M. Q., L. Duval, C. Chaux, and J.-C. Pesquet, 2014, A primal-dual proximal algorithm for sparse template-based adaptive filtering: Application to seismic multiple removal: IEEE Trans. Signal Process., **62**, 4256–4269.

Repetti, A., M. Q. Pham, L. Duva, E. Chouzenoux, and J.-C. Pesquet., 2015, Euclid in taxicab: sparse blind deconvolution with smoothed ℓ_1/ℓ_2 regularization: IEEE signal processing letters, **22**, 539–543.

Ricker, N., 1940, The form and nature of seismic waves and the structure of seismogram: Geophysics, **5**, 348–366.

Riel, P. V., and A. J. Berkhout, 1985, Resolution in seismic trace inversion by parameter estimation: Geophysics, **50**, 1440–1455.

Taylor, H. L., S. C. Banks, and J. F. McCoy, 1979, Deconvolution with the ℓ_1 norm: Geophysics, **44**, 39–52.

Tibshirani, R. J., 2013, The LASSO problem and uniqueness: Electronic Journal of Statistics, **7**, 1456–1490.

Ulrych, T., 1971, Application of homomorphic deconvolution to seismology: Geophysics, **36**, 650–660.

Wang, Y., 2002, A stable and efficient approoach of inverse Q filtering: Geophysics, **67**, 657–663.

———, 2008, Seismic inverse Q-filtering: Blackwell Pub.

Zhang, C., and T. Ulrych, 2002, Estimation of quality factors from CMP record: Geophysics, **67**, 1542–1547.

Zhang, R., and J. Castagna, 2011, Seismic sparse-layer reflectivity inversion using basis pursuit decomposition: Geophysics, **76**, 147–158.